

Solid Lipid Nanoparticles Encapsulating Naturally Derived Boschniakine Mitigates Induced Diabetic Nephropathy

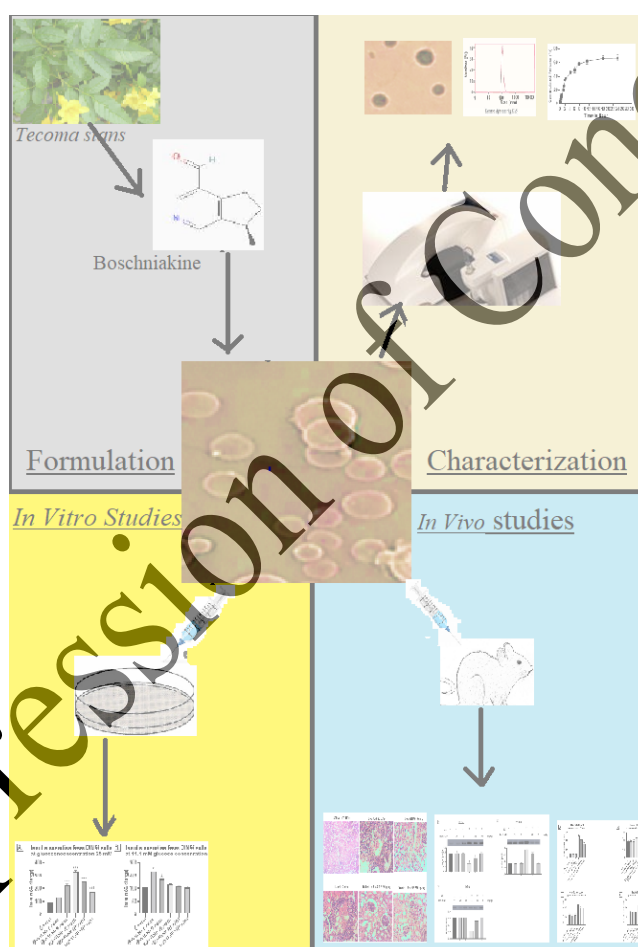
Adriel A. Ekozin^{a*}, Michele Senrubolo^b, Christopher M. Pam^c, Oladutun B. Isola^a

^aDepartment of Chemical Sciences, College of Basic and Applied Sciences, Glorious Vision University, Ogwa, Edo State Nigeria.

^bDepartment of Chemistry, University of Cambridge, Cambridge, U.K.

^cInstitute of Structural and Molecular Biology, University College London, U.K.

Graphical Abstract



Abstract

Boschniakine, a bio-alkaloid isolated from the *Tecoma stans* plant, has been reported to be traditionally utilized for the management of diabetes in model systems through multiple biochemical mechanisms. Studies on boschniakine are sparse, considering that poor absorption, a rapid metabolic rate, and systemic elimination could limit bio-alkaloids' pharmacological efficacy. We propose using highly bioavailable boschniakine-solid lipid nanoparticles (Bos-SLNPs) to recognize such limitations. This study examined the potential molecular mechanisms underlying the anti-diabetic effects of Bos-SLNP. Bos-SLNP (25 and 50 mg/kg) was evaluated for 30 days for its anti-diabetic activity in streptozotocin-

* Corresponding author: ekozinadriel@gmail.com

induced Type 1 and Type 2 diabetic rats. In addition, the RT-polymerase chain reaction technique was used to determine the messenger-RNA expression of Interleukin-1, Interleukin-6, and Tumor Necrosis Factor- α in renal tissue. Hematoxylin and eosin staining and Western blotting were used to find differences in the nuclear factor erythroid 2-related factor 2/heme oxygenase/Nuclear factor- κ B signaling pathway and how its proteins were expressed. Bos-SLNP treatment increased the expression of nuclear factors erythroid 2-related factor 2 and heme oxygenase-1 and decreased the expression of Nuclear factor-B. This was because Bos-SLNPs have a protective mechanism from their anti-inflammatory and antioxidant properties. Bos-SLNPs exhibited a protective effect against diabetic nephropathy in rats induced with streptozocin, possibly via the nuclear factor erythroid 2-related factor pathway 2 / heme oxygenase 1/ nuclear factor kappa B.

Keywords

Boschniakine-SLNPs, Diabetes Nephropathy, Nrf2, HO-1

Rationale, Purpose, and Limitations

Tecoma stans, traditionally used for diabetes management (Costantino et al., 2003), contain significant concentrations of boschniakine chemicals, a naturally occurring pyridine carboxaldehyde compound. The molecular mechanisms behind boschniakine's antihyperglycemic properties remain unclear. To address issues of drug-candidate half-life, bioavailability, and solubility, we coupled boschniakine to solid lipid nanoparticles. This study aims to determine the attenuating impact of boschniakine-solid lipid nanoparticles (Bos-SLNPs) on diabetic nephropathy induced by streptozotocin (STZ) nicotinamide. Additionally, we investigate the effect of Bos-SLNPs on diabetic nephropathy (DN) induced by streptozotocin (STZ)-cadmium preparations. The research is constrained by its restricted timeframe. Additionally, it is imperative to conduct extended testing over an extended duration to substantiate these observations before advancing to clinical trials.

Introduction

Diabetes mellitus (DM) is a metabolic disorder marked by hyperglycemia (elevated blood sugar levels) and insulin resistance. Currently, 366 million people are living with diabetes, and experts anticipate this number to increase by 2030 (Aziz & Ahsan Ali, 2020). Tangvarasittichai (2015) suggests that the development of DM may result in the excessive production of ROS beyond the physiological threshold, negatively impacting the cardiovascular system, nervous system, kidneys, and eyes. DN is among several complications associated with both type 1 and type 2 diabetes, involving changes in the extracellular matrix of renal tis-

sues, abnormal mesangial enlargement, glomerulosclerosis, and tubulointerstitial renal fibrosis (Das et al., 2021).

The release of heavy metals into the environment due to human industrial activity poses a significant health concern. Cadmium (Cd), one such heavy metal, can cause substantial damage to the kidneys. Research indicates that a weekly intake of no more than 7 μ g/kg of cadmium is considered safe for humans (Satarug et al., 2020). Nevertheless, concentrations beyond these thresholds may be surpassed due to environmental pollution. Streptozotocin (STZ)-prone rat models are more susceptible to Cd-induced kidney damage than control animals (Gungor & Kara, 2020), and prolonged exposure to Cd has been linked to impaired blood filtration through the glomerulus (Fujishiro et al., 2019; Jain, 2020). Consequently, there is a pressing need for drugs that can lower blood sugar levels and protect against heavy metal toxicity. Researchers are actively investigating the therapeutic potential of plants, leveraging their bioactive constituents to attenuate diseases and mitigate the adverse impacts associated with exposure to toxic metals (Mihailović et al., 2021).

To prevent Cd toxicity in diabetic rats, studying immune and inflammatory responses in STZ-induced rat models is crucial. Nuclear factor erythroid 2-related factor 2 (Nrf 2) has been identified as a key biomolecule involved in cell defense, metabolism, immune response, and maintaining the cell cycle. Nrf 2 safeguards the kidneys through the neutralization of ROS, and the strategic utilization of the Nrf 2/heme oxygenase-1 signaling pathway is suggested as an approach to addressing diabetes nephropathy (Luo et al., 2022; Ulasov et al., 2022).

Experimental

Materials and methods

Chemicals and animals

STZ was procured from Sigma Chemical Co. (St Louis, MO, USA), while rabbit polyclonal COX-2 antibodies were acquired from Cayman Chemical Co. (Ann Arbor, MI, USA). Zymed Laboratories (San Francisco, CA, USA) provided anti-rabbit, anti-goat, and anti-mouse horseradish peroxidase-conjugated secondary antibodies. The ARE oligonucleotide was sourced from Bionics (Seoul, Korea), and Amersham Pharmacia Biotech supplied the enhanced chemiluminescence (ECL) detection kit and [γ - 32 P] ATP (Buckinghamshire, UK). All remaining reagents were obtained in the highest commercially available purity.

Adult male rats weighing 180–200 g were sourced from the primate colony at the University of Ibadan's Department of Veterinary Pathology in Ibadan, Nigeria. These rats received commercial pelleted food (Ladokun Feeds, Ibadan, Nigeria) and free water access. They were housed under standard laboratory conditions and exposed to a natural photoperiod of 12 h light/12 h dark. The humane treatment of all animals was ensured following the standards for laboratory animal management outlined by the Redeemer's University Committee on Ethics for Scientific Research (Number 13489). Stainless steel cages maintained a constant temperature of 25°C for the animals.

Plant collection

In January 2022, leaf specimens of *Tecoma stans* (Juss) (Bignoniaceae) were collected at the University of Ibadan, Ibadan, Oyo State, Nigeria, specifically at Sauder Road. A voucher specimen (LC-2022/01) has been securely deposited at the Herbarium of the Nigerian Forest Research Institute.

Extraction of boschniakine

The dried leaves (500 g) were extracted using the Soxhlet method with $C_4H_{10}O/NH_3$ 15% (10/90 v/v). After extracting the organic layer with 4 N HCl (1000 ml), the aqueous phase was washed with ether (3×200 mL), basified with 30% NH_3 , and extracted with CH_2Cl_2 (2×500 mL). The organic layer was then dried (Na_2SO_4), and the solvent was removed at decreased pressure. The crude alkaloidic fraction

obtained was subsequently subjected to chromatography on silica gel, employing CH_2Cl_2 and progressively increasing quantities of CH_3OH (ranging from 0% to 40%). Boschniakine was eluted at 2% CH_3OH (TLC mobile phase $CH_2Cl_2/CH_3OH/NH_3$ 89.5/10/0.5, R_f 0.9). Boschniakine was identified by direct comparison of the 1H nuclear magnetic resonance (NMR), ^{13}C NMR, and electron ionization (EI)-mass spectral results with previously published data (Costantino et al., 2003).

Boschniakine-solid lipid nanoparticles

Preparation

Boschniakine-solid lipid nanoparticles (Bos-SLNPs) were synthesized using the microemulsion technique Li et al. (2020) outlined with slight modifications. A mixture comprising 45.45% polysorbate 80, 0.58% PLPC (1-Palmitoyl-2-linoleoyl-sn-glycero-3-phosphocholine), and water was subjected to heating in a beaker until reaching the lipid's melting point. The lipid component (7.27%) experienced dissolution, with an average melting temperature of 82°C. The lipid (7.27%) underwent melting at an average temperature of 82°C. Subsequently, boschniakine (25 mg) was suspended in an aqueous phase containing polysorbate 80 and added directly to the melted lipid, achieving complete dissolution. Magnetic stirring was employed to generate a transparent microemulsion. The resulting mixture was transferred to a heated microemulsion with an equivalent volume of cold water (2°C). The procedure was executed under mechanical stirring at a speed of 5000 rpm using an IKA C-MAG HS 7 Magnetic stirrer for 1.5 hours. The formation of Bos-SLNPs was observed through the crystallization and microemulsion of the heated lipid droplets. The Bos-SLNP product was refrigerated for subsequent investigations.

Characterization studies of Bos-SLNPs

Employing the dynamic light scattering technique, Nano-ZS ZEN 3600 was utilized to assess the polydispersion (PDI), zeta potential, mean size, and size distribution of Bos-SLNPs. Scattering frequency was determined at 90° and 25° angles. The size of the Bos-SLNPs was ascertained through transmission electron microscopy (TEM). The morphology of the Bos-SLNPs was analyzed using scanning electron microscopy (SEM).

Evaluation of Bos-SLNPs encapsulation effectiveness

The methodology outlined by Li et al. [14], with minor modifications, was employed to determine the encapsulation efficiency of the nanoformulation, represented as the percentage of boschniakine entrapped within the nanoparticles. After dissolving 25 mg of Bos-SLNPs in 1 mL of 90% methanol for 5 minutes, the solution underwent sonication to disrupt the nanoparticles and release the encapsulated boschniakine. The resultant solution was centrifuged at $10,000 \times g$ to isolate the supernatant. Quantification of boschniakine was conducted by spectrophotometric analysis of the supernatant using a Shimadzu (1601 UV/VIS) spectrophotometer.

In vitro Bos-SLNPs release

Bos-SLNPs were subjected to in vitro release profiling using a dialysis bag technique. In succinct terms, a 25 mg suspension of Bos-SLNPs in phosphate-buffered saline (PBS) (2 mL) was introduced into a dialysis bag with a molecular weight cutoff ranging from 12,000 to 14,000 Da. The dialysis bag opening was securely fastened with pins and immersed in a bottle containing 50 mL of phosphate buffer saline (pH 7.4) with 1% polysorbate 80, maintained under continuous agitation at 100 rpm. At 1-hour intervals, 1 mL of PBS was withdrawn and spectrometric assessments of boschniakine were conducted at 425 nm. Following each withdrawal, 1 mL of fresh PBS was introduced into the container to maintain fluid conditions.

Insulin secretion study

RIN5f cells were cultured at 37°C with 5% CO₂ in Roswell Park Memorial Institute (RPMI) medium, which included 4.5 g/L glucose, 1% antibiotic solution, and 10% fetal bovine serum. These cells were seeded at a density of 4×10^5 cells/mL in a 24-well microtiter plate. After 72 hours, the medium was replaced, and another 48 hours later, the medium without fetal bovine serum was substituted. Subsequently, Bos-SLNPs suspensions in saline were duplicated and applied to specific wells at final concentrations of 1, 3, 10, 30, and 100 g/mL. After 4 hours, cell supernatants were collected, centrifuged, and stored at -20 °C until further analysis. The Rat/Mouse Insulin ELISA Kit (Millipore Corp., MA, USA) was employed to assess insulin concentration in the supernatants.

Similarly, insulin secretion was evaluated in RIN5f cells cultured in RPMI media containing 2 g/L glucose.

Animal treatment

Male albino Wistar rats were procured from the primate colony within the Department of Veterinary Pathology at the University of Ibadan, Ibadan, Nigeria. These rats were acclimatized to a temperature-controlled environment (25°C) with a 12-hour light/12-hour dark cycle for 5 days. The animals were provided with a standard diet and unrestricted access to water. Approval for the experimental procedures was obtained in adherence to the guidelines governing the handling of laboratory animals, as specified by the Glorious Vision University Committee on Ethics for Scientific Research (Approval No. GVU/ACH/2023-6).

Induction of types 1 & 2 diabetes in rats

Preceding the commencement of experimental protocols the rats were randomly allocated into four distinct experimental groups: the normal control group (N group, 10 rats), the STZ control group (D group, 10 rats), the STZ + glibenclamide group (G + D, 10 rats), the STZ + Bos-SLNP group at a dose of 25 mg/kg body weight (D + B group), and the STZ + Bos-SLNP group at a dose of 50 mg/kg body weight (D + B group). Type 1 diabetes was induced intraperitoneally by administering streptozotocin at a dosage of 50 mg/kg, prepared in a 0.1 M citrate buffer with a pH of 4.4 [15]. For the induction of type 2 diabetes, streptozotocin (90 mg/kg) was intraperitoneally administered to rat pups at 5 days old, and they were allowed to develop until 12 weeks of age [16,17]. They were given Cd as CdCl₂ at 100 ppm concentration dissolved in drinking water [16]. Animals displaying hyperglycemia (glucose levels of 250–500 mg/dL) were randomly assigned to one of the five groups (n = 10). Simultaneously, the control group (n=10) received an equivalent volume of citrate buffer.

Single-dose oral glucose tolerance test studies in types 1 & 2 diabetic rats

For 18 hours, diabetic rats were starved. Oral administration of Bos-SLNP (5, 25, and 50 mg/kg) and 0.1 M citrate buffer with a pH of 4.4 was used to treat and control rats. Following 1 hour of ether anesthesia, blood samples were obtained from the retroorbital plexus, and glucose levels were assessed using the Accu-

Chek® Active Blood Glucose Meter System (Roche Diagnostics, Mannheim, Germany). Subsequently, each rat received an oral glucose load of 1.5 g/kg body weight (time of administration recorded as '0' min). Blood samples were collected at 30-, 60-, and 120-minute intervals, and glucose levels were analyzed.

Repeated-dose studies in types 1 & 2 diabetic rats

A citrate buffer solution with a concentration of 0.1 M and a pH of 4.4 was administered to nondiabetic and diabetic control group rats. Bos-SLNP was administered to rats in the treatment group at doses. Rats were dosed orally once daily on a bodyweight basis for four weeks. Food and water intake were monitored daily. On day 28, blood samples (500 L) were collected from nonfasted rats 1 hour after treatment, and glucose levels were determined. Centrifugation was used to separate serum (150 L), which was then kept at -20 °C and tested for insulin levels using a rat insulin ELISA kit. The following day, rats fasted for 18 hours and were exposed to an oral glucose tolerance test (OGTT). At each time point of the OGTT, blood glucose levels were assessed.

Repeated-dose studies in types 1 & 2 diabetic rats

A citrate buffer solution with a concentration of 0.1 M and a pH of 4.4 was administered to nondiabetic and diabetic control group rats. Bos-SLNPs were administered to rats in the treatment group at doses. Rats were dosed orally once daily on a bodyweight basis for four weeks. Food and water intake were monitored daily. On day 28, blood samples (500 L) were collected from nonfasted rats 1 hour after treatment, and glucose levels were determined. Centrifugation was used to separate serum (150 L), which was then kept at -20 °C and tested for insulin levels using a rat insulin ELISA kit. The following day, rats fasted for 18 hours and were exposed to an OGTT. At each time point of the OGTT, blood glucose levels were assessed.

Repeated-dose studies in types 1 & 2 diabetic rats

The nondiabetic and diabetic control groups received 0.1 M citrate buffer with a pH of 4.4.

In the treatment group, Bos-SLNP (administered to rats at specific doses). Rats were orally dosed once daily over four weeks based on body weight. Daily monitoring included assessing food and water intake. On day 28, nonfasted rats had blood samples (500 µL) collected 1 hour after treatment, and glucose levels were determined. Serum (150 µL) was separated via centrifugation, stored at -20°C, and subsequently analyzed for insulin levels using a rat insulin ELISA kit. The following day, rats underwent an 18-hour fasting period and were subjected to an OGTT. At each time point during the OGTT, blood glucose levels were measured.

Superoxide dismutase (SOD), catalase (CAT), and malondialdehyde (MDA) measurement in renal tissue

Anesthesia was induced in the animals via intraperitoneal administration of thiopental (100 mg/kg) and lidocaine (10 mL/kg). Subsequently, an abdominal incision was made to collect blood, and exsanguination was performed. Vital organs were extracted for further analysis. Serum triglycerides (TG), non-esterified fatty acids (NEFA), and total cholesterol levels in renal tissues were assessed using standard kits from the same samples (Randox Laboratories, Crumlin, UK) (Umrani & Paknikar, 2014). The preserved renal tissue samples were used to determine the activity of SOD and catalase using kits from Cayman Chemical (MI, USA).

qRT-PCR

Total RNA was extracted from kidney samples prepared using the guanidinium thiocyanate reagent. Complementary DNA synthesis was done through reverse transcription (RT) following the manufacturer's protocol. Subsequently, we employed a standard in developing quantitative real-time polymerase chain reaction (qRT-PCR). Gene-specific PCR amplification was performed using the ABI 7300 and the Synergy Brands, Inc. green PCR kit. Relative gene expression levels were calculated using the 2- $\Delta\Delta C_t$ methodology after normalizing to GAPDH messenger-RNA levels. The following primers were utilized in real-time PCRs:

1. TNF- α :
Forward: 5'-ACTTTGGAGTGATCGGCCCC-3'
Reverse: 5'-TTCTGTGTGCCAGACACCCTA-3'
2. IL-6:
Forward: 5'-CCTTCTCCACAATACCCCCAGG-3'
Reverse: 5'-TGTGCCAGTGGACAGGTTT-3'
3. IL-1 β :
Forward: 5'-ACCTGAGCTCGCCAGTGAAAT-3'
Reverse: 5'-ACCCTAAGGCAGGCAGTTGG-3'
4. GAPDH:
Forward: 5'-TGGGGTGATGCAGGTGCTAC-3'
Reverse: 5'-GGACAGGAAGGCCATACCA-3'

Histopathological changes

The kidney tissue was longitudinally harvested, fixed in 4% paraformaldehyde, and subsequently embedded in paraffin. Sections of 4 μ m thickness were prepared, stained with H&E staining, and examined under an optical microscope. Deep coronal sections were scrutinized, and the percentage of kidney involvement assessed the severity of damage. The evaluation, conducted with the assistance of a microscope, involved grading based on parameters such as tubular cell necrosis, cytoplasmic vacuole formation, hemorrhage, and tubular dilatation. The extent of damage was quantified in ten regions corresponding to the renal proximal tubules.

Western blot

For the western blot analysis, 150 μ g protein aliquots from the kidney tissue supernatant were subjected to separation on a 10% SDS-PAGE gel. Inhibition was performed with 3% bovine serum albumin in 0.2% to 0.4% TBST for one hour. Subsequently, the membranes were incubated overnight at 4°C with primary antibodies targeting active TAT-14 Peptide, Heme Oxygenase-1, and NF κ B, followed by incubation with alkaline phosphatase-conjugated secondary antibodies. Membranes were visualized using 5-bromo-4-chloro-3-indolyl phosphate/nitroblue tetrazolium, and the blots were stained with an anti-actin antibody. Protein concentrations were normalized relative to the actin band density. Thermo Scientific Super Signal West Pico Chemiluminescent Substrate was utilized to quantify the antigen-antibody products, and the results were analyzed using a Fluor Chem system (Sharma et al., 2013).

Statistical analysis

The data were expressed as mean \pm SEM. The data were also analyzed using ANOVA to evaluate the difference between the groups using Tukey's multiple comparison test (significance p value $<$ 0.05).

Discussion

Plants are currently investigated for their bioactive components, particularly in diabetes nephropathy management (Lei et al., 2022). Strategies involving bioactive components from plants have been proposed to address the complexities of diabetes nephropathy. Given the susceptibility of individuals with diabetes to cadmium toxicity, focusing on signaling molecule responses emerges as a promising approach to target molecular pathways that mediate inflammation and DN (Aziz & Ahsan Ali, 2020; Phoenix et al., 2022). Due to the well-established association between inflammation and diabetes, targeted inhibition of intracellular signaling pathways involved in the inflammatory response is now considered a promising strategy for developing molecular target-based chemopreventive agents (Hu et al., 2021). Consequently, modulation of the cellular signaling network, specifically the Nrf2/HO-1/NF- κ B induction, and activity, is recognized as a novel paradigm for preventing nephropathy, with this signaling pathway identified as a key factor in nephropathy prevention (Heeba et al., 2022; Ding et al., 2022).

Isolation of boschniakine

Boschniakine compounds were isolated from *Tecoma stans*, resulting in a yield of 0.7 g of oil with purity (determined by GC) exceeding 96%. The specific rotation ($[\alpha]$) in CHCl₃ was measured as +22.58 (C = 1), corresponding to

an optical rotation of +21°. Infrared spectroscopy (IR) analysis (Nujol) revealed peaks at 1697 cm^{-1} . Proton nuclear magnetic resonance (^1H NMR) in CDCl_3 exhibited signals at 1.38 (3H, d, J 6.91), 1.60–1.84 (1H, m), 2.36–2.54 (1H, m), 3.00–3.48 (3H, m), 8.62 (1H, s), 8.83 (1H, s), and 10.23 (1H, s), as per the findings reported by IMAKURA et al., (1985).

Characterization of prepared Bos-SLNPs

Tecoma stans has a historical application in modern clinical medicine for diabetes treatment, with Tecomine compounds identified as

the active anti-diabetic fraction of *Tecoma stans* (Costantino et al., 2003; Al-Azzawi et al., 2012; Ha et al., 2022). Boschniakine, an alkaloid isolated from *Tecoma stans*, was encapsulated within SLNPs using the microemulsion technique. The resulting Bos-SLNPs demonstrated a transparent microemulsion with enhanced benefits compared to boschniakine alone. The morphology and distribution of the synthesized Bos-SLNPs were assessed through SEM, TEM, and dynamic light scattering.

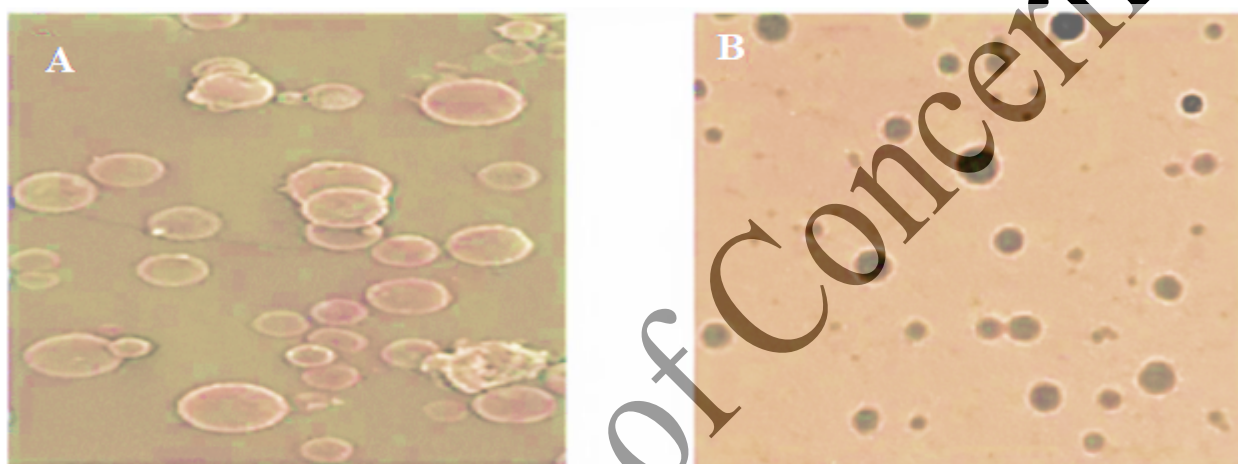


Figure 1. (A) SEM micrographs of the Bos-SLNPs, (B) TEM image of Bos-SLNPs.

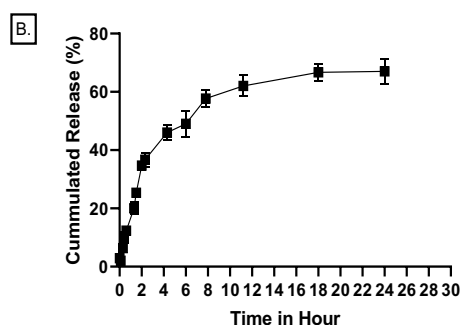
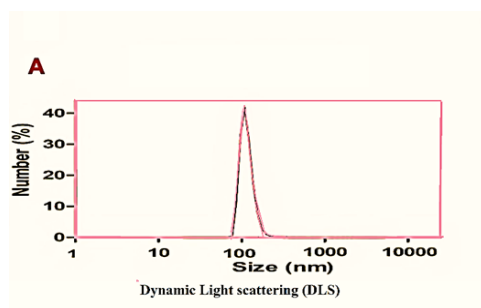


Figure 2. (A) DLS analysis of the boschniakine-SLNPs, and (B) In vitro release profile of boschniakine-SLNPs. DLS = dynamic light scattering; SLNPs = solid lipid nanoparticles; STZ = streptozotocin.

As depicted in Figures 1A and B and 2A and B, the Bos-SLNPs exhibited a diminutive, compact spherical structure, featuring an average particle size of 152.7 ± 7.04 nm. The zeta potential was measured at 52.18 ± 3.90 mV, and the polydispersity index (PDI) was found to be 0.692. The encapsulation efficiency of Bos-SLNPs was determined to be 78.90%. In the context of Bos-SLNP, Figure 2B illustrates the

drug release profile over time. The average release rate of Bos-SLNP during 24 hours was 71.52%, with a rapid release rate of 34.28% observed within the initial 5 hours. Subsequently, the release percentage exhibited a gradual increase over the 24-hour duration.

Insulin secretion study

Boschniakine-SLNPs were further explored for their impact on glucose-stimulated insulin secretion (GSIS). The study revealed that Bos-

SLNPs increased insulin secretion dose-dependently in the RIN5f cell line, indicating potential insulin secretagogue properties without inducing hypoglycemia. Administration of Bos-SLNPs demonstrated a dose-dependent increase in insulin secretion by RIN5f cells

treated with a glucose concentration of 25 mM, compared to untreated cells (observed as a 3.5-fold increase at 10 $\mu\text{g}/\text{mL}$ Bos-SLNP concentrations, Figure 3A).

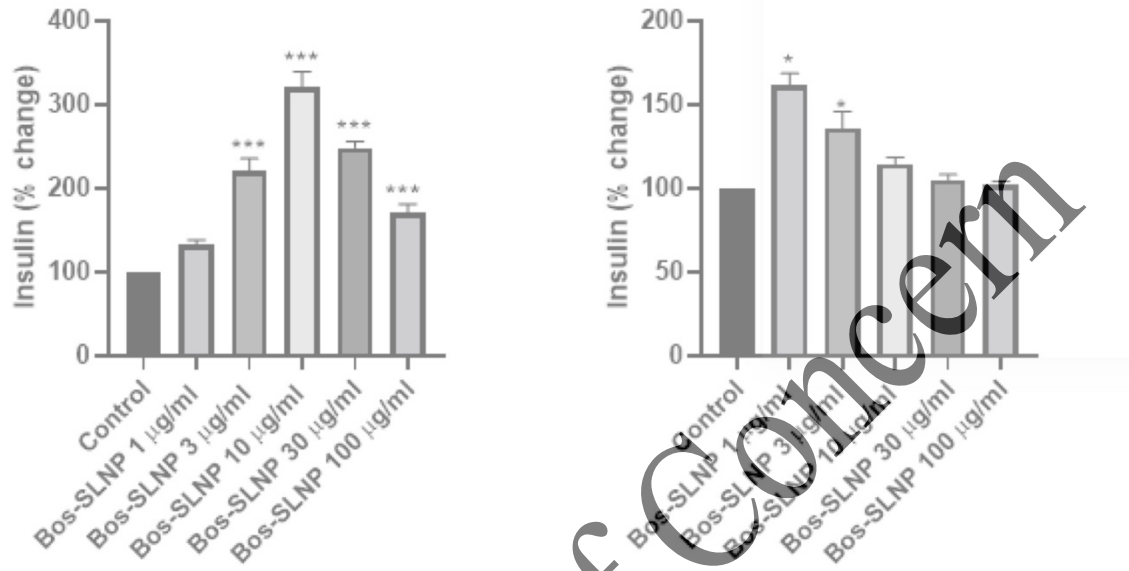


Figure 3. Insulin secretion from RIN5f cells after 4 h of exposure to different concentrations of Bos-SLNPs; cells maintained at (A) 25 mM and (B) 11.1 mM glucose concentration.

However, higher concentrations of Bos-SLNPs (30 and 100 $\mu\text{g}/\text{mL}$) reduced insulin secretion. Under 11.1 mM glucose conditions, insulin production by RIN5f cells remained nearly constant across a range of Bos-SLNP concentrations (Figure 3B).

Administration of Bos-SLNPs at doses of 25 and 50 mg/kg exhibited a reduction in blood glucose levels in type 1 diabetic rats at the 30- and 60-minute time points, as depicted in Figure 4A. However, statistical significance was not observed.

Single-dose OGTT studies in types 1 & 2 diabetic rats

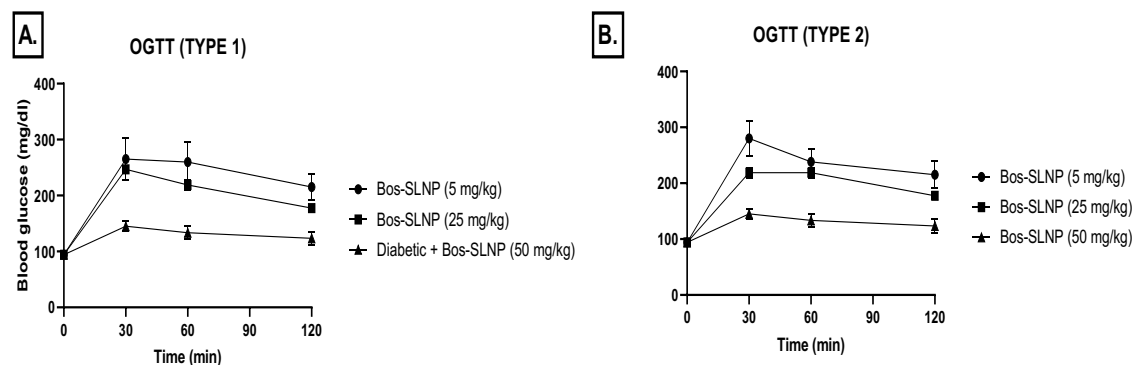


Figure 4. Oral glucose tolerance test results after a single administration of Bos-SLNPs. (A) Blood glucose levels of type 1 diabetic rats and (B) Blood glucose levels of type 2 diabetic rats.

Bos-SLNP therapy decreased glucose levels in type 2 diabetic rats during the OGTT, as illustrated in Figure 4B. In single-dose OGTT studies, Bos-SLNP administration demonstrated significant glucose suppression, suggesting anti-diabetic properties. Similar findings were documented by Ramachandran et al. (2019).

Repeated-dose OGTT studies in types 1 & 2 diabetic rats

In repeated dosing studies, diabetic control rats demonstrated the anticipated elevation in fasting blood glucose levels and glucose intolerance. The treatment of type 1 diabetic rats with Bos-SLNPs resulted in a substantial reduction in both nonfasted and fasted blood glucose levels, demonstrating reductions of 20% and 26%, respectively, with a 50 mg/kg dose (refer to Figures 5A and 5B).

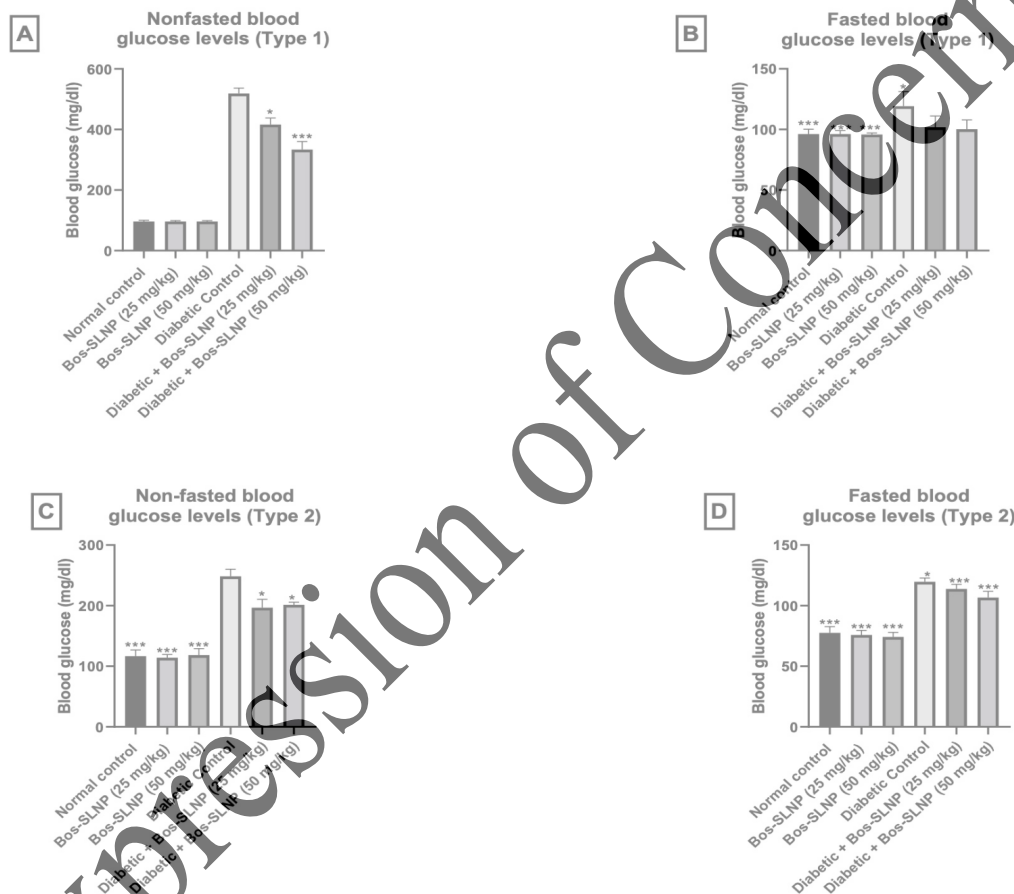


Figure 5. Anti-diabetic activity of Bos-SLNPs (4 weeks of treatment) in diabetic rats. (A) Nonfasted blood glucose levels (type 1); (B) fasted blood glucose levels (type 1); (C) Nonfasted blood glucose levels (type 2); (D) fasted blood glucose levels (type 2)

Additionally, Bos-SLNP therapy exhibited a significant decrease in hyperglycemia in type 2 diabetic rats, showcasing reductions of 29% and 21% in nonfasted and fasting blood glucose levels, respectively, at a dose of 10 mg/kg (refer to Figures 5C and 5D). Administering Bos-SLNP multiple times to diabetic rats led to more significant improvements in glucose intolerance compared to single-dose studies, underscoring the enhanced effectiveness of multiple

dosages. Furthermore, the suppression of glucose levels during the OGTT was more pronounced in rats with type 2 diabetes than in those with type 1 diabetes. This disparity may be attributed to the lower β -cell mass observed in Wistar rats with type 1 diabetes (Abels et al., 2022), potentially resulting in diminished GSIS.

The administration of Bos-SLNP to diabetic rats resulted in a significant reduction in both

nonfasted and fasted blood glucose levels. The decline in nonfasting glucose levels signifies an augmentation of GSIS. This reduction in nonfasted glucose levels was more prominent in type 2 diabetic rats compared to type 1 diabetic rats and exhibited a direct correlation with elevated serum insulin levels. The observed inhibitory effects of Bos-SLNP on glycogenolysis and gluconeogenesis, activities prominent during the fasting state, were indicated by a decrease in fasting glucose levels. Consequently, inhibiting glucagon-stimulated hepatic pathways, specifically glycogenesis and gluconeogenesis, in the fasting state (Zhang et al., 2022) contributed to decreased fasting glucose levels. Comparable observations regarding the anti-diabetic activity of berberine-loaded SLNPs were made by Xue et al. (2013).

The administration of Bos-SLNP to diabetic rats increased insulin levels, indicative of insulin secretagogue activity. In our investigation, the observed elevation in insulin levels was notably significant under nonfasted conditions, whereas no significant change was observed under fasted conditions. This potential glucose-dependent secretagogue effect of Bos-SLNP holds promise, as it may mitigate the risk of hypoglycemia. The positive impact of Bos-SLNP on triglyceride (TG) and nonesterified fatty acid (NEFA) levels suggests insulin-mimetic effects in adipocytes.

Superoxide dismutase (SOD), catalase (CAT), and MDA measurement in renal tissue

The recognized imbalance between oxidants and antioxidants is acknowledged to induce oxidative stress. ROS accumulation can interfere with polyunsaturated fatty acids, leading to lipid peroxidation in renal tissues and eventually causing damage and toxicity (Allam et al., 2022). Oxidative stress is widely recognized as the primary cause of complications associated with diabetes, including neuropathy (Sharma et al., 2021; Gandhi et al., 2022). ROS can degrade membrane polyunsaturated fatty acids, generating 4-Hydroxynonenal (4-HNE) and MDA, an unstable aldehyde capable of forming covalent protein compounds—a hallmark of oxidative stress-induced tissue injuries. SOD and catalase serve as crucial free radical scavenging enzymes, constituting the initial defense against oxidative damage in mammals. Superoxide dismutase (SOD) converts superoxide radicals (O_2^-) into molecular O_2 and hydrogen peroxide. The relationship between SD, malondialdehyde, and DN has been well-established. SOD, catalase, and MDA assessments were employed to evaluate lipid peroxidation. The induction of STZ significantly diminished the activity of SD and catalase ($p < 0.001$), as outlined in Table 1.

Table 1. Effects of Bos-SLNPs on MDA, SOD, CAT, TG, and Serum NEFA

Treatment Groups	MDA (nmol/mg prot)	SOD (U/mg prot)	CAT (U/mg prot)	TG (Mg/dL)	NEFA (Mg/dL)
Normal Control	1.93 ± 0.04	79.61 ± 3.28	17.27 ± 1.72	44.13 ± 3.02	0.38 ± 0.02
Bos-SLNP (25 mg/kg)	1.89 ± 0.11c	73.21 ± 2.15c	16.72 ± 2.02c	38.74 ± 8.82	0.41 ± 0.01c
Bos-SLNP (50 mg/kg)	1.90 ± 0.23c	78.32 ± 3.08c	17.07 ± 2.02c	40.14 ± 3.22	0.44 ± 0.07c
Diabetic Control	4.89 ± 0.18z	20.88 ± 1.04z	6.03 ± 1.00z	57.65 ± 6.56z	0.93 ± 0.05z
Diabetic + Bos-SLNP (25 mg/kg)	3.05 ± 0.18a	58.26 ± 3.29b	10.04 ± 1.72a	31.70 ± 2.15	0.76 ± 0.06a
Diabetic + Bos-SLNP (50 mg/kg)	2.02 ± 0.50c	72.90 ± 3.81c	14.28 ± 1.04b	39.10 ± 4.82	0.54 ± 0.04b

*Values are expressed as means ± SD. Compared with control: zP < 0.001; compared with streptozocin: aP < 0.05, bP < 0.01 and cP < 0.001.

MDA = malondialdehyde; SOD, CAT = catalase; TG = triglyceride; NEFA = nonesterified fatty acid.

Subsequently, Bos-SLNPs at 25 and 50 mg/kg doses effectively restored superoxide dismutase and catalase levels ($p < 0.05$, 0.01 , and 0.001). Moreover, streptozocin therapy led to an increase in MDA levels ($p < 0.001$). Conversely, administering Bos-SLNPs at 25 and 50 mg/kg doses significantly reduced MDA levels (p values < 0.05 , 0.01 , and 0.001). Similarly, STZ-induced elevations in serum triglyceride and non-esterified fatty acid (NEFA) levels were observed. However, Bos-SLNPs at 25 and 50 mg/kg doses successfully restored the altered levels. Catalase, a prominent antioxidant in the kidneys, is pivotal in eliminating hydrogen peroxide and shielding tissues from reactive hydroxyl radicals (Ekozin et al., 2022). Past research has demonstrated that catalase deficiency, attributed to peroxisome deficiency, accelerates kidney damage in type 1 diabetes. Our study affirms the role of Bos-SLNPs in augmenting the activity of SD and catalase while

reducing malondialdehyde levels in the renal tissues of STZ-stimulated rats.

Interleukin-6, interleukin-1, and tumor necrosis factor-alpha mRNA expression in response to boschniakine-SLNPs

The mRNA expression levels of interleukin-6, tumor necrosis factor-alpha, and Interleukin-1 were significantly heightened ($p < 0.001$) in rats treated with STZ compared to control rats. However, administering Bos-SLNPs to STZ-pretreated rats significantly decreased the mRNA expression of interleukin-6, tumor necrosis factor-alpha, and interleukin-1 ($p < 0.05$, 0.01 , and 0.001). Notably, the sole administration of Bos-SLNPs did not induce any alterations in the mRNA expression of interleukin-6, tumor necrosis factor-alpha, or interleukin-1, as illustrated in Figure 6.

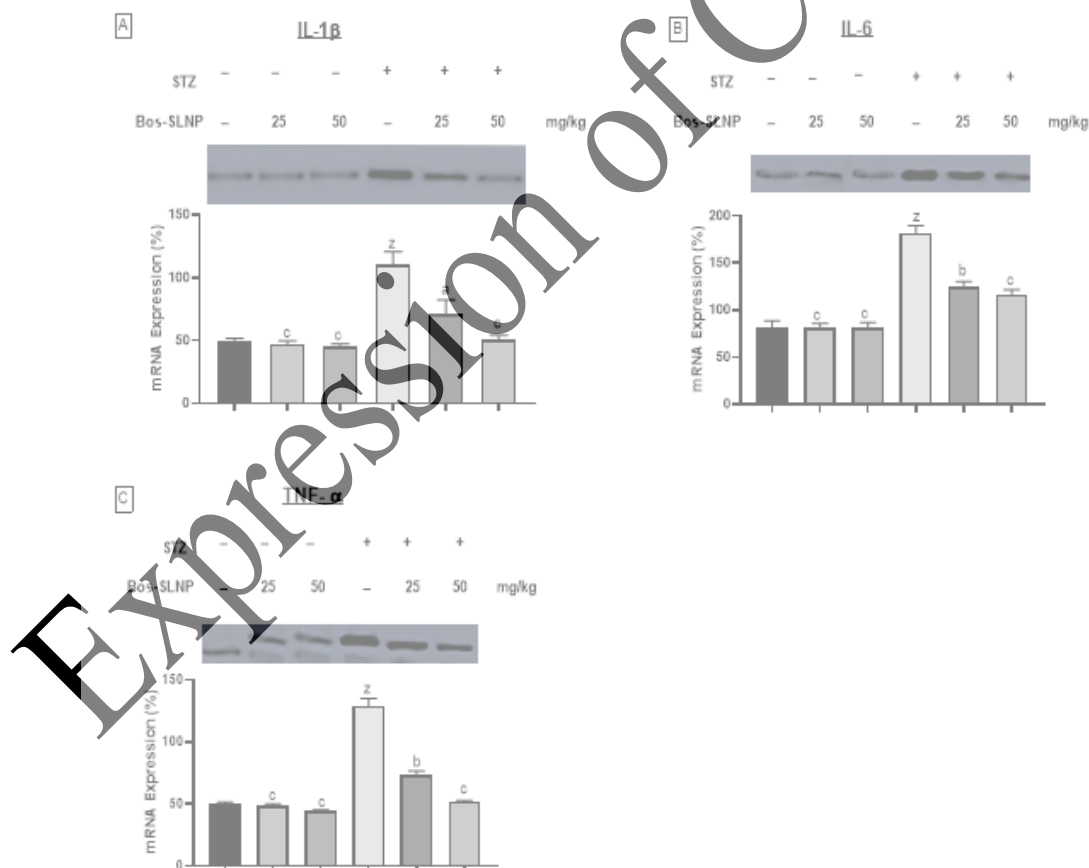


Figure 6. Effect of Bos-SLNPs on the expression of inflammatory cytokines (IL-1 β , IL-6, and TNF- α) in the kidney of STZ-treated rats. Quantifications of IL-1 β (A), IL-6 (B) and TNF- α (C). Lane 1, control; Lane 2, Bos-SLNPs (25 mg/kg); Lane 3, Bos-SLNPs (50 mg/kg); Lane 4, diabetic control; Lane 5, Bos-SLNPs (25 mg/kg) plus Diabetic control; Lane 6, Bos-SLNPs (25 mg/kg) plus Diabetic control. Compared with control: ^z $P < 0.001$; compared with STZ: ^a $P < 0.05$, ^b $P < 0.01$ and ^c $P < 0.001$.

Furthermore, the mRNA expression levels of cytokines in renal tissues corroborated the anti-inflammatory efficacy of Bos-SLNPs. In the renal tissues of diabetic rats, there was a significant elevation in the mRNA levels of interleukin-6, tumor necrosis factor, and interleukin-1 β . However, treatment with Bos-SLNPs resulted in a reduction of these levels to that observed in normal rats. Previous studies have elucidated the pivotal role interleukin-6 in leukocyte recruitment, apoptosis, and T-lymphocyte activation (Belaid et al., 2021; Alam et al., 2021). Tumor necrosis factor is recognized for its ability to stimulate the transcription and release of cytokines and chemokines by neutrophils (Éva Sikura et al., 2021). Inhibiting the release of tumor necrosis factor- α , interleukin-1, and interleukin-6 may effectively attenuate inflammation.

TAT-14 peptide, NF- κ B, and heme oxygenase-1 proteins expression in response to Bos-SLNPs

Nuclear factor- κ B (NF- κ B) is a key player in the pathophysiology of DN in rats, characterized by inflammation and oxidative stress. The

expression levels of tumor necrosis factor- α , interleukin-1, and interleukin-6 positively correlate with the activation of NF- κ B. The up-regulation of interleukin-10, facilitated by the ability of heme oxygenase-1 to catabolize free heme and produce carbon monoxide, underscores its inherent anti-inflammatory property. Nuclear factor erythroid 2-related factor 2 (Nrf2) serves as a pivotal regulator of the anti-oxidative defense pathway, activated in response to diabetes and DN (Wang et al., 2021). Bos-SLNPs administered at doses of 25 and 50 mg/kg exhibited no discernible impact on the expression levels of NF- κ B, TAT-14 peptide, and heme oxygenase-1 in rats compared to the control group. In contrast, diabetic control rats displayed a significant increase in NF- κ B expression, accompanied by a notable decrease in the expressions of Nrf2 and HO-1 relative to control rats ($P < 0.001$). However, as depicted in Figure 7, Bos-SLNPs at doses of 25 and 50 mg/kg effectively attenuated the altered protein expression of NF- κ B, TAT-14 peptide, and heme oxygenase-1 in STZ-induced diabetic rats (p values of 0.05, 0.01, and 0.001).

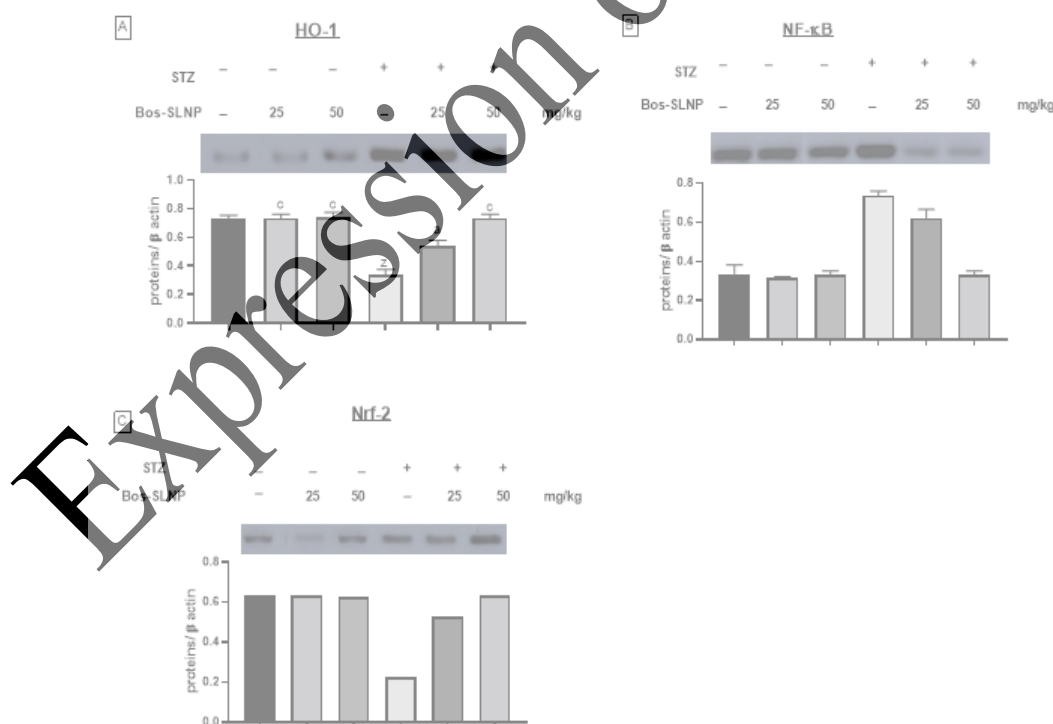


Figure 7. Effect of Bos-SLNPs on the protein's Nrf2, NF- κ B, and HO-1 expression in the kidney tissue. Quantifications of HO-1 (A), NF- κ B (B), and Nrf-2 (C). Lane 1, control; lane 2, Bos-SLNPs (25 mg/kg); lane 3, Bos-SLNPs (50 mg/kg); lane 4, diabetic control; lane 5, Bos-SLNPs (25 mg/kg) plus diabetic control; lane 6, Bos-SLNPs (25 mg/kg) plus diabetic control. compared with control: $^aP < 0.001$; compared with STZ: $^bP < 0.05$, $^cP < 0.01$ and $^dP < 0.001$.

Furthermore, the mRNA expression levels of cytokines in renal tissues corroborated the anti-inflammatory efficacy of Bos-SLNPs. In the renal tissues of diabetic rats, there was a significant elevation in the mRNA levels of interleukin-6, tumor necrosis factor, and interleukin-1 β . However, treatment with Bos-SLNPs resulted in a reduction of these levels to that observed in normal rats. Previous studies have elucidated the pivotal role of interleukin-6 in leukocyte recruitment, apoptosis, and T-lymphocyte activation (Belaid et al., 2021; Alam et al., 2021). tumor necrosis factor is recognized for its ability to stimulate the transcription and release of cytokines and chemokines by neutrophils (Éva Sikura et al., 2021). Inhibiting the release of tumor necrosis factor- α , interleukin-1, and interleukin-6 may effectively attenuate inflammation.

Nuclear factor- κ B (NF- κ B) is a key player in the pathophysiology of DN in rats, characterized by inflammation and oxidative stress. The expression levels of tumor necrosis factor- α , interleukin-1, and interleukin-6 positively

correlate with the activation of NF- κ B. The up-regulation of interleukin-10, facilitated by the ability of heme oxygenase-1 to catabolize free heme and produce carbon monoxide, underscores its inherent anti-inflammatory property. Nrf2 serves as a pivotal regulator of the antioxidative defense pathway, activated in response to diabetes and DN (Wang et al., 2021).

Previous studies have shown that enhancing the Nrf2/heme oxygenase-1 pathway inhibits apoptosis and that Nrf2 can increase heme oxygenase-1 expression (Zhang et al., 2022). In rats with DM, the expression of Nrf2 and heme oxygenase-1 was down-regulated, whereas the expression of nuclear factor- κ B was up-regulated. Bos-SLNP treatment increased Nrf2 and HO-1 expression and decreased NF- κ B activity, indicating that Bos-SLNP protection is based on its anti-inflammatory activity by decreasing the development of LFO by preventing the release of pro-inflammatory factors and its antioxidant activity, which is likely dependent on controlling activated IL-6, IL-1, TNF, and NF- κ B via the Nrf2/HO-1 signaling pathway in DN induced by STZ.

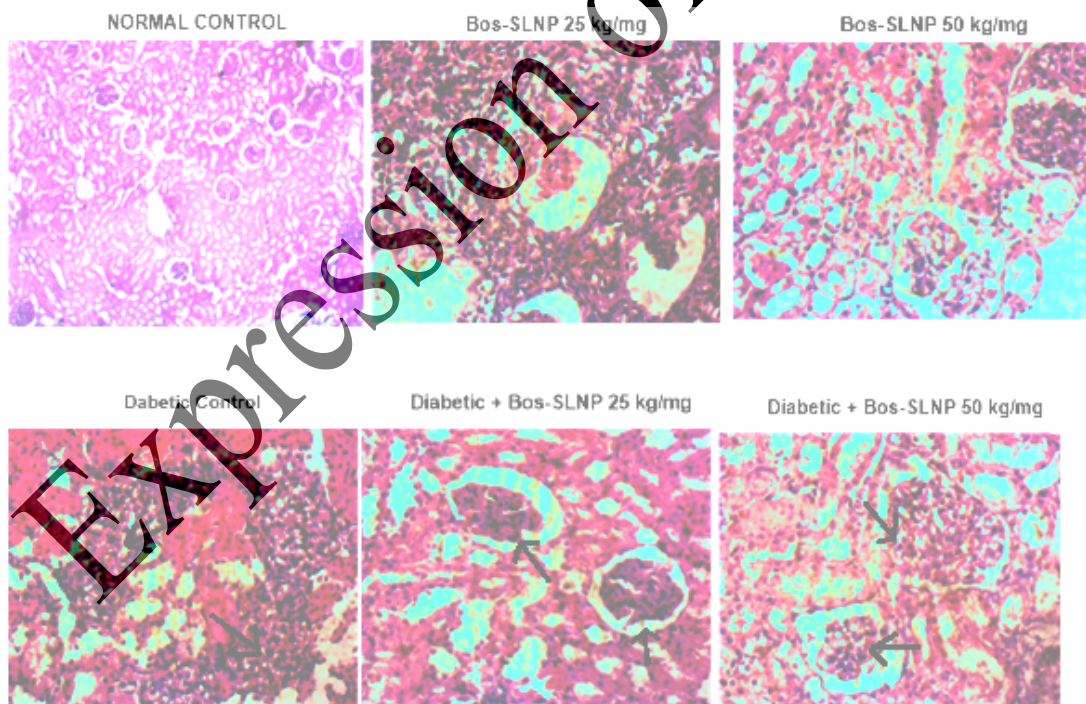


Figure 8. Boschniakine-SLNPs (Bos-SLNPs) effect on histopathological changes of renal tissue. H&E staining of kidney sections. The kidney from control revealed normal cell architecture. Diabetic control showed extreme tubular necrosis, mild glomerular dilation, and interstitial inflammation. Bos-SLNPs 25 and 50 mg/kg (D and E) revealed normal cell architecture.

Bos-SLNPs effect on renal tissue histopathology

Histological evaluation utilizing H&E staining was employed to assess the protective efficacy of Bos-SLNPs against physiological dysfunction. Renal tissue examination in the control group exhibited a typical cell architecture.

Conclusion

Taken together, the ability of Bos-SLNP to inhibit ROS formation and inflammation is possibly through the Nrf2/heme oxygenase-1/nuclear factor- κ B signaling pathway. In view of the present study, Bos-SLNPs merit further consideration for exploring clinical application in the chemoprevention of diabetic nephropathy.

Author Contributions

Adriel Ekozin: Conceptualization, Investigation, Methodology, Data curation. Adriel Ekozin, Ishola Bamiji, Michele Senrubolo, and Christopher M. Pam: Animal experiment. Adriel Ekozin, Michele Senrubolo, Ishola Bamiji, and Christopher M. Pam: ELISA, Western Blotting analyses and Writing-original draft. Adriel Ekozin, Michele Senrubolo, and Christopher M. Pam conducted experiments and analyzed the data results. Adriel Ekozin, Michele Senrubolo: Writing-revising and editing.

Ethics Statement

The experimental protocol reviewed and approved the animal study and was conducted according to the Laboratory Animal Research Center of Glorious Vision University, Ogwa, Edo State, Nigeria (Approval No. GVV-BCH-2022-6).

Conflict of interest

The authors declare no conflict of interest. For a signed statement, please contact the journal office at editor@precisionnanomedicine.com.

Data Availability Statement

The data used in the current study are available from the corresponding author upon reasonable request.

Quote this article as Ekozin AA, Senrubolo M, Pam CM, Bamiji I, Solid Lipid Nanoparticles Encapsulating Naturally Derived Boschniakine Mitigates Induced Diabetic Nephropathy, *Precis. Nanomed.* 2023, 6(4):1194-1210, <https://doi.org/10.332/001c.xxxxx>

COPYRIGHT NOTICE ©The Author(s) 2024. This article is distributed under the terms of the Creative Commons Attribution 4.0 International License, which permits unrestricted use, distribution, and reproduction in any medium, provided you give appropriate credit to the original author(s) and the source, provide a link to the Creative Commons license, and indicate if changes were made.

References

- Z. Zhang, B. Yan, Y. Li, S. Yang, and J. Li, "Propofol inhibits oxidative stress injury through the glycogen synthase kinase 3 beta/nuclear factor erythroid 2-related factor 2/heme oxygenase-1 signaling pathway," *Bioengineered*, vol. 13, no. 1, pp. 1612–1625, 2022. doi:10.1080/21655979.2021.2021062
- J. Wang *et al.*, "Association of Nuclear Factor erythroid-2-related actor 2 gene polymorphisms with diabetic nephropathy in Chinese patients," *International Journal of General Medicine*, vol. Volume 14, pp. 1231–1237, 2021. doi:10.2147/ijgm.s300152
- K. Éva Sikura *et al.*, "Hydrogen sulfide inhibits aortic valve calcification in heart via regulating runx2 by NF-KB, a link between inflammation and mineralization," *Journal of Advanced Research*, vol. 27, pp. 165–176, 2021. doi:10.1016/j.jare.2020.07.005
- [4] M. S. Alam *et al.*, "TNF plays a crucial role in inflammation by signaling via T cell TNFR2," *Proceedings of the National Academy of Sciences*, vol. 118, no. 50, 2021. doi:10.1073/pnas.2109972118

- [5] B. Belaid *et al.*, “T cell counts and IL-6 concentration in blood of North African covid-19 patients are two independent prognostic factors for severe disease and death,” *Journal of Leukocyte Biology*, vol. 111, no. 1, pp. 269–281, 2021. doi:10.1002/jlb.4cova1020-703r
- [6] K. Éva Sikura *et al.*, “Hydrogen sulfide inhibits aortic valve calcification in heart via regulating runx2 by NF-KB, a link between inflammation and mineralization,” *Journal of Advanced Research*, vol. 27, pp. 165–176, 2021. doi:10.1016/j.jare.2020.07.005
- [7] J. Wang *et al.*, “Association of Nuclear Factor erythroid-2-related actor 2 gene polymorphisms with diabetic nephropathy in Chinese patients,” *International Journal of General Medicine*, vol. Volume 14, pp. 1231–1237, 2021. doi:10.2147/ijgm.s300152
- [8] A. Ekozin, C. A. Otuechere, and A. Adewuyi, “Apocynin loaded silver nanoparticles displays potent in vitro biological activities and mitigates pyrogallol-induced hepatotoxicity,” *Chemico-Biological Interactions*, vol. 365, p. 110069, 2022. doi:10.1016/j.cbi.2022.110069
- [9] M. Gandhi, E. Fargo, L. Prasad-Reddy, K. M. Mahoney, and D. Isaacs, “Diabetes: How to manage diabetic peripheral neuropathy,” *Drugs in Context*, vol. 11, pp. 1–13, 2022. doi:10.7571/dic.2021-10-2
- [10] S. Sharma, P. Vas, and G. Rayman, “Small fiber neuropathy in diabetes polyneuropathy: Is it time to change?,” *Journal of Diabetes Science and Technology*, vol. 16, no. 2, pp. 311–331, 2021. doi:10.1177/1932296821996434
- [11] A. Allam *et al.*, “N-acetylcysteine alleviated the deltamethrin-induced oxidative cascade and apoptosis in liver and kidney tissues,” *International Journal of Environmental Research and Public Health*, vol. 19, no. 2, p. 638, 2022. doi:10.3390/ijerph19020638
- [12] M. Xue *et al.*, “Characterization, pharmacokinetics, and hypoglycemic effect of berberine loaded solid lipid nanoparticles,” *International Journal of Nanomedicine*, p. 4677, 2013. doi:10.2147/ijn.s51262
- [13] T. Zhang, J. Zhang, H. Wang, and P. Li, “Correlations between glucose metabolism of bone marrow on 18F-fluoro-D-glucose pet/computed tomography and hematopoietic cell populations in autoimmune diseases,” *Nuclear Medicine Communications*, vol. 44, no. 3, pp. 212–218, 2022. doi:10.1097/mnm.0000000000001657
- [14] M. Abels *et al.*, “Overexpressed beta cell cart increases insulin secretion in mouse models of insulin resistance and diabetes,” *Peptides*, vol. 151, p. 170747, 2022. doi:10.1016/j.peptides.2022.170747
- [15] V. Ramachandran *et al.*, “Antidiabetic activity of gold nanoparticles synthesized using wedelolactone in rin-5f cell line,” *Antioxidants*, vol. 9, no. 1, p. 8, 2019. doi:10.3390/antiox9010008
- [16] K.-N. Ha *et al.*, “Alpha-glucosidase inhibitors from *Nervilia concolor*, *Tecoma Stans*, and *Bouea macrophylla*,” *Saudi Journal of Biological Sciences*, vol. 29, no. 2, pp. 1029–1042, 2022. doi:10.1016/j.sjbs.2021.09.070
- [17] A. Al-Azzawi, K. Al-Samerai, E. Al-Khateeb, and A. Al-Juboori, “Antibacterial activity and the histopathological study of crude extracts and isolated tecomine from *Tecoma Stans* Bignoniaceae in Iraq,” *Pharmacognosy Research*, vol. 4, no. 1, p. 37, 2012. doi:10.4103/0974-8490.91033
- [18] L. Costantino *et al.*, “Isolation and pharmacological activities of the *Tecoma stans* alkaloids,” *Il Farmaco*, vol. 58, no. 9, pp. 781–785, 2003. doi:10.1016/s0014-827x(03)00133-2
- [19] B. Ding *et al.*, “Corrigendum to ‘berberine reduces renal cell pyroptosis in golden hamsters with diabetic nephropathy through the Nrf2-NLRP3-caspase-1-GSDMD pathway,’” *Evidence-Based Complementary and Alternative Medicine*, vol. 2022, pp. 1–1, 2022. doi:10.1155/2022/9828973
- [20] G. H. Heeba, M. A. Ali, and A. A. El-Sheikh, “Rosuvastatin induces renal HO-1 activity and expression levels as a main protective mechanism against STZ-induced diabetic nephropathy,” *Medicina*, vol. 58, no. 3, p. 425, 2022. doi:10.3390/medicina58030425
- [21] Z. Hu *et al.*, “Glycyrrhizin regulates rat TMJOA progression by inhibiting the HMGB1-Rage/TLR4-NF-KB/Akt Pathway,” *Journal of Cellular and Molecular Medicine*, vol. 26, no. 3, pp. 925–936, 2021. doi:10.1111/jcmm.17149
- [22] A. Phoenix, R. Chandran, and A. Ergul, “Cerebral microvascular senescence and inflammation in diabetes,” *Frontiers in Physiology*, vol. 13, 2022. doi:10.3389/fphys.2022.864758

- [23] C. Argano *et al.*, “An overview of systematic reviews of the role of vitamin D on inflammation in patients with diabetes and the potentiality of its application on diabetic patients with COVID-19,” *International Journal of Molecular Sciences*, vol. 23, no. 5, p. 2873, 2022. doi:10.3390/ijms23052873
- [24] L. Lei *et al.*, “Morus alba L. (sangzhi) alkaloids promote insulin secretion, restore diabetic β -cell function by preventing dedifferentiation and apoptosis,” *Frontiers in Pharmacology*, vol. 13, 2022. doi:10.3389/fphar.2022.841981
- [25] Y. IMAKURA *et al.*, “Studies on constituents of Bignoniaceae plants. iv. isolation and structure of a new iridoid glucoside, campside, from *Campsis chinensis*,” *Chemical and Pharmaceutical Bulletin*, vol. 33, no. 6, pp. 2220–2227, 1985. doi:10.1248/cpb.33.2220
- [26] A. K. Sharma *et al.*, “Dual therapy of vildagliptin and Telmisartan on diabetic nephropathy in experimentally induced type 2 diabetes mellitus rats,” *Journal of the Renin-Angiotensin-Aldosterone System*, vol. 15, no. 4, pp. 410–418, 2013. doi:10.1177/1470320313475908
- [27] R. D. Umrani and K. M. Paknikar, “Zinc oxide nanoparticles show anti-diabetic activity in streptozotocin-induced type 1 and 2 diabetic rats,” *Nanomedicine*, vol. 9, no. 1, pp. 99–104, 2014. doi:10.2217/nmm.12.205
- [28] P. Li *et al.*, “Apigenin-loaded solid lipid nanoparticle attenuates diabetic nephropathy induced by streptozotocin nicotinamide through Nrf2/HO-1/NF-KB signalling pathway,” *International Journal of Nanomedicine*, vol. Volume 15, pp. 9115–9124, 2020. doi:10.2147/ijnm.s56494
- [29] L. Costantino *et al.*, “Isolation and pharmacological activities of the *Tecoma stans* alkaloids,” *Il Farmaco*, vol. 58, no. 9, pp. 781–785, 2003. doi:10.1016/s0014-827x(03)00133-2
- [30] A. V. Ulasov, A. A. Rosenkranz, G. P. Georgiev, and A. S. Solovlev, “Nrf2/KEAP1/Are Signaling: Towards specific regulation,” *Life Sciences*, vol. 291, p. 120111, 2022. doi:10.1016/j.lfs.2021.120111
- [31] H. Luo, Z. Bao, M. Zhou, Y. Chen, and Z. Huang, “Notoginsenoside R1 alleviates spinal cord injury by inhibiting oxidative stress, neuronal apoptosis, and inflammation via activating the nuclear factor erythroid 2 related factor 2/heme oxygenase-1 signaling pathway,” *NeuroReport*, vol. 33, no. 11, pp. 451–462, 2022. doi:10.1097/wnr.0000000000001903
- [32] M. Mihailović *et al.*, “The influence of plant extracts and phytoconstituents on antioxidant enzymes activity and gene expression in the prevention and treatment of impaired glucose homeostasis and diabetes complications,” *Antioxidants*, vol. 10, no. 3, p. 480, 2021. doi:10.3390/antiox10030480
- [33] R. B. Jain, “Cadmium and kidney function: Concentrations, variabilities, and associations across various stages of glomerular function,” *Environmental Pollution*, vol. 256, p. 113361, 2020. doi:10.1016/j.envpol.2019.113361
- [34] H. Fujishiro, S. Hamada, M. Isawa, and S. Himeno, “Segment-specific and direction-dependent transport of cadmium and manganese in immortalized S1, S2, and S3 cells derived from mouse kidney proximal tubules,” *The Journal of Toxicological Sciences*, vol. 44, no. 9, pp. 611–619, 2019. doi:10.2131/jts.44.611
- [35] H. Gungor and H. Kara, “Effects of selenium, zinc, insulin and metallothionein on cadmium-induced oxidative stress and metallothionein gene expression levels in diabetic rats,” *Journal of Basic and Clinical Pharmacology and Pharmacology*, vol. 31, no. 2, 2020. doi:10.1515/jbcpp-2019-0198
- [36] S. Satarug, G. C. Gobe, D. A. Vesey, and K. R. Phelps, “Cadmium and lead exposure, nephrotoxicity, and mortality,” *Toxics*, vol. 8, no. 4, p. 86, 2020. doi:10.3390/toxics8040086
- [37] F. Li *et al.*, “High glucose-stimulated enhancer of zeste homolog-2 (EZH2) forces suppression of deceptor to cause glomerular mesangial cell pathology,” *Cellular Signalling*, vol. 86, p. 110072, 2021. doi:10.1016/j.cellsig.2021.110072
- [38] S. Tangvarasittichai, “Oxidative stress, insulin resistance, dyslipidemia and type 2 diabetes mellitus,” *World Journal of Diabetes*, vol. 6, no. 3, p. 456, 2015. doi:10.4239/wjd.v6.i3.456
- [39] A. Aziz and S. Ahsan Ali, “Compliance of checking hba1c in a Tertiary Care Hospital of Pakistan,” *Pakistan Journal of Medical Sciences*, vol. 37, no. 1, 2020. doi:10.12669/pjms.37.1.2814